FET-Based Planar Circuits for Quasi-Optical Sources and Transceivers

JOEL BIRKELAND, STUDENT MEMBER, IEEE AND TASUO ITOH, FELLOW, IEEE

Abstract — **We describe the design and construction of planar FET-based quasi-optical sources and transceivers. The circuits are quite simple in construction and exhibit isotropic conversion gain. Both single-device and balanced transmitter and transceiver circuits are described. Balanced sources are reported which may be operated in push–pull mode for power combining or in push–push mode for frequency doubling. A single-FET quasi-optical oscillator circuit using a microstrip patch linear array is reported with an effective radiated power of 31.6 dBm at 10 GHz. A dual-FET frequency-doubling oscillator circuit using a coupled rampart line antenna is reported with an effective radiated power of 21.6 dBm at 19.7 GHz. Quasi-optical transceiver elements are reported which use the FET's as both signal sources and self-oscillating mixers for down-conversion of the received signal. The application of these transceiver elements to Doppler motion detection is reported.**

I. Introduction

THE USE OF planar circuits for the generation and combination of microwave power has received attention in the past few years [1]–[6]. One application is in the area of quasi-optical systems, in which traditional microwave guiding structures such as hollow waveguide and microstrip are replaced by free-space propagation using wave beam modes [1]. Such systems are useful at millimeter-wave frequencies. Another application is active antenna elements for radar and communication systems [4]–[7]. In this case planar circuits have the advantage of light weight and small volume, and the ability to conform to different surface profiles.

In this paper we present planar GaAs MESFET based circuits for the generation, transmission, and reception of microwave power. In these circuits, oscillators are formed by coupling FET's to microstrip leaky-wave antennas which function as both resonator and radiating elements. This approach is similar to the one using Gunn diodes and dielectric waveguide described by Song and Itoh [8]. The resulting circuits are quite simple and can be used as elements in active arrays. For transceiver operation, the oscillating FET, in addition to supplying the transmitted energy, also operates as a self-oscillating mixer for down-conversion of the received signal.

Manuscript received December 21, 1988; revised April 1, 1989. This work was supported by the Texas Advanced Technology Program and by the U.S. Army Research Office under Contract DAAL03-88-K-005.

The authors are with the Department of Electrical and Computer Engineering, University of Texas at Austin, Austin, TX 78712.

IEEE Log Number 8929187.

The choice of GaAs MESFET's (or, alternatively, HEMT's) for the active elements in our designs is quite reasonable. The FET is currently the workhorse in MMIC designs. In general, FET's also show a higher dc–RF conversion efficiency than diode sources. Finally, it is reasonable to expect that FET performance will continue to improve at millimeter-wave frequencies.

The leaky-wave antennas which are used in these circuits consist of periodic linear microstrip arrays. Operation in the broadside radiating mode occurs in conjunction with very high *VSWR*; this is often referred to as the leaky-wave stopband. In conventional antenna applications this situation is avoided. However, in our present application we use this high *VSWR* (in the vicinity of 10:1 for the antennas discussed here) to our advantage: the antenna functions as a frequency-selective element which reflects energy back to the FET, thereby sustaining oscillation. In this way, the antenna operates as both the resonant and the radiating element in our circuit.

The design and performance of prototype circuits which operate in *X*-band as sources and transceivers are presented here. Two basic types of circuits are described: single-ended structures, in which one FET drives a linear microstrip patch array, and balanced structures, where two devices are operated in either a push–pull mode for power combining or a push–push configuration for frequency doubling. The circuits are characterized by isotropic conversion gain. Qualitative performance of transceiver circuits for Doppler motion detection applications is also presented.

II. Circuit Elements

The basic circuit which we use is a negative resistance oscillator, which consists of two parts: an active portion, which provides the negative resistance, and a passive portion, which is the resonant element and selects the frequency of oscillation. The active part includes the FET and its corresponding bias circuitry, and the passive part consists of the microstrip resonant antenna.

A. The Active Element

If we use the simple linear model for the FET in Fig. 1, shown with the source grounded and the gate terminated in a reactance B_g, we may derive the following expression

0018-9480/89/0900-1452$01.00

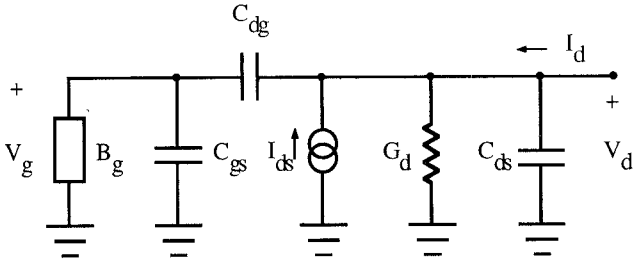

Fig. 1. A one-port circuit formed from an equivalent circuit for the FET by grounding the source and terminating the gate in a reactive load.

for the admittance at the drain port:

$$Y_d = \frac{I_d}{V_d} = \frac{\omega g_m C_{dg}}{B_g + \omega C_{gs} + \omega C_{dg}} + G_d + j\omega\left[C_{dg}\left(\frac{B_g + \omega C_{gs}}{B_g + \omega C_{gs} + \omega C_{dg}}\right) + C_{ds}\right].$$

This expression indicates that, by terminating the gate port of the device in the proper admittance, the admittance at the drain will become negative. In this case, we may view the FET as a one-port negative resistance device. In addition, since the FET uses a Schottky-type gate contact, C_{gs} varies with V_{gs}, indicating that the frequency of oscillation of the final circuit may be varied by changing the gate voltage.

The choice of the gate circuit is dictated by the properties of the remainder of the oscillator circuit. In order to reduce the possibility of oscillation at a frequency other than that which is desired, it may be necessary to design the gate circuit to appear as a reactance at the desired operating frequency, and as a resistive termination at other frequencies.

B. The Resonant Element

The resonant elements in our circuits are microstrip linear arrays which operate in a region of high *VSWR* referred to as the leaky-wave stopband, in which the radiation is perpendicular to the direction of propagation, i.e., normal to the plane of the microstrip substrate. The origins of this phenomenon may be understood by considering the $k_0d-\beta d$ diagram of an electromagnetic wave on an infinite periodic structure [9].

For waves propagating in a basically slow guiding structure with an infinitesimal periodic perturbation, $k_0d-\beta d$ appears as shown in Fig. 2. The area of the diagram where $k_0d > \beta d$ is called the fast wave region, where radiation from an open guiding structure may occur; the region where $k_0d < \beta d$ is called the slow wave region. At the points where the curves representing the forward-traveling and backward-traveling waves cross, mode coupling occurs, creating stopbands. In the stopband regions, the coupling to the backward space harmonic creates high *VSWR* on the structure.

As the frequency is increased from low values, the first stopband encountered is at point A, where the β_0 and $-\beta_{-1}$ space harmonics are coupled. This is the so-called surface wave stopband since it occurs in the slow wave

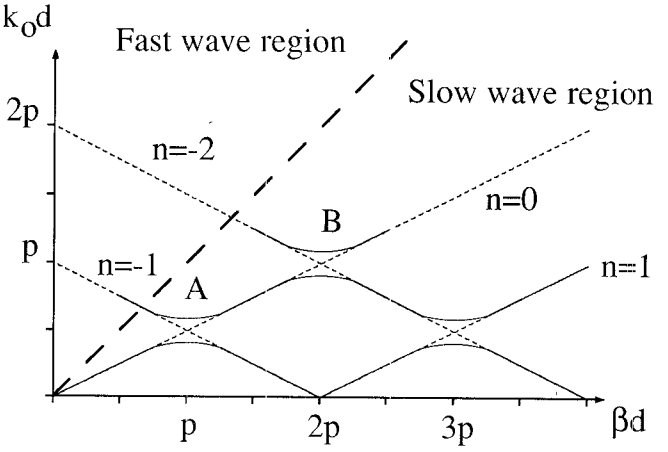

Fig. 2. The $k_0d-\beta d$ diagram

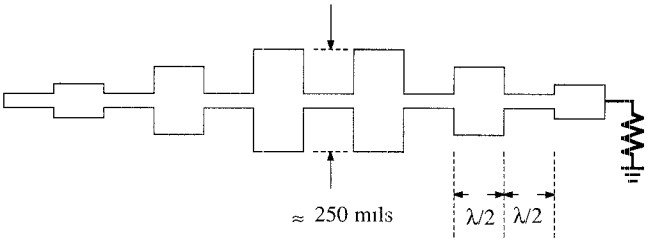

Fig. 3. Microstrip patch linear array.

region of the $k_0d-\beta d$ diagram. The next stopband is encountered at the point B, and is due to the coupling between the β_0 and $-\beta_{-2}$ space harmonics. At the same time, the $-\beta_{-1}$ space harmonic is in the fast wave region and radiates in the broadside direction. This is the "leaky-wave" stopband, and it is in this region that we are interested in operating.

The preceding discussion involved only the general form of the dispersion curves in the limit of an infinitesimal perturbation. In practice, some of the space harmonics and stopbands may be missing due to additional symmetry of the structure. In addition, the presence of higher order modes are not taken into account.

III. Oscillator Design

Two basic types of circuits have been constructed: the single-device and the balanced oscillator. The balanced oscillator type may be used in the power-combining mode or the frequency-doubling mode, depending on whether the FET's oscillate in the even or the odd mode. We consider the two types separately.

A. Single-Device Design

The single-device circuit uses a periodic microstrip patch linear array as the resonant element. This type of circuit is described in greater detail in [10]; a review is given here.

The microstrip patch linear array, shown in plan view in Fig. 3, consists of varying width patch elements of length $\lambda/2$ separated by sections of 50 Ω line of length $\lambda/2$, where λ is the wavelength in the microstrip. The widths of the patch elements increase from the ends of the array to a maximum value in the center. The structure is terminated

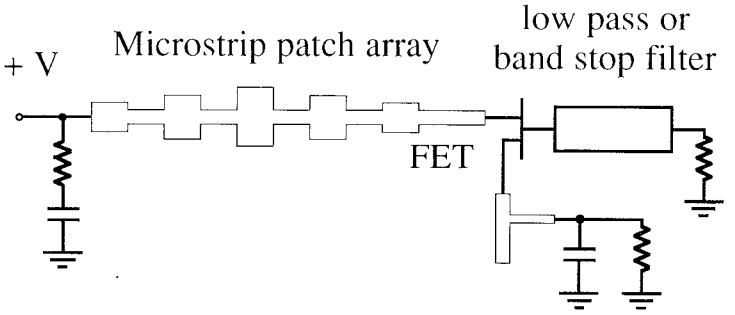

Fig. 4. Schematic view of single-device oscillator circuit.

in a 50 Ω resistor. The radiation from the step discontinuities can be considered to arise from an equivalent magnetic current sheet in the transverse plane from the end of the patch element to ground. The radiated E field will therefore be polarized along the axis of the antenna.

The antenna was fabricated using Rogers Duroid 6010.2 with a thickness of 25 mils and a relative dielectric constant of 10.2. The following empirical design approach was taken: The widest patch elements, in the center of the structure, were given widths slightly greater than $\lambda/2$ to maximize the radiation without permitting higher order modes [11]; the element lengths were determined by taking into account fringing fields. Actual values for these elements were $w = 250$ mils and $l = 192$ mils. The widths of the remaining elements were decremented in both directions for the overall resonator. The tapered profile of the structure was optimized using the Touchstone CAD program from EEsof in terms of its performance as a resonant element, taking into account parasitic elements.

A schematic view of the single-device oscillator circuit is shown in Fig. 4. The gate of the device is terminated in a band-stop filter which provides the correct reactance at the oscillation frequency, while appearing as a resistive termination at lower frequencies, to prevent oscillation in the surface wave stopband.

B. Balanced Oscillator

With the balanced approach, the oscillator may be designed for operation in either the push–pull mode for power combining or the push–push mode for frequency doubling. The push–push oscillator is described here for the first time; preliminary results for the push–pull design appear in [12].

The balanced oscillator also uses a periodic distributed resonator, except that in this case the resonator is a two-port coupled rampart line antenna. This type of antenna consists of two rampart line antennas placed side by side, as shown in Fig. 5. For angles close to normal, the radiation from this type of antenna may be considered to arise from a magnetic current source located along the mitered edge [13]. If the excitation frequency, f_0, is such that the electrical distance between the centers of the miters is $\lambda/4$, the antenna will radiate in the broadside direction, with the electric field polarized perpendicular to its length. If the excitation frequency is $2f_0$, the electrical distance between the centers of the miters is $\lambda/2$, and the antenna will also radiate in the broadside direction, but the polarization will be parallel to the axis of the antenna. For this reason, when a signal consisting of a fundamental f_0 plus a second harmonic at $2f_0$ is applied to the ports of the antenna in the odd mode, the fundamental signal is radiated and the second harmonic is suppressed. Alternatively, when the same signal is applied in the even mode, the second harmonic is radiated and the fundamental is suppressed. This latter condition is the basis for the push–push frequency-doubling circuit described below.

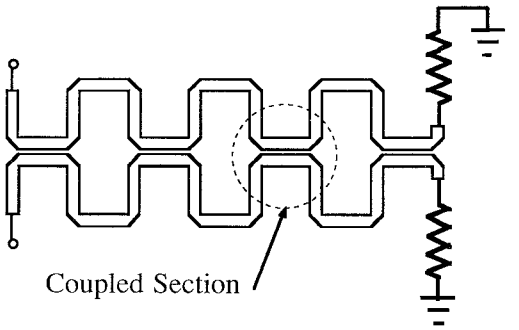

Fig. 5. Four-section coupled rampart line array.

The coupled sections, which exhibit even- and odd-mode impedances Z_{0e} and Z_{0o}, are separated by three equal-length sections, each having characteristic impedance Z_0. Z_{0e} and Z_{0o} depend on the width and spacing of the two constituent lines. If we choose the widths and spacings of the coupled sections so that $Z_{0o} < Z_0$ and $Z_{0e} = Z_0$, then reflective stopbands will exist in the odd mode due to the periodic impedance variations, but none will occur in the even mode. Similarly, if we have $Z_{0o} = Z_0$ and $Z_{0e} > Z_0$, then the stopbands will occur in the even mode. In addition, the widths and spacings of the coupled sections may be varied from section to section, to alter the shape of the stopband.

The push–pull and push–push circuits were fabricated using Rogers Duroid 5880 with a thickness of 20 mils and a relative dielectric constant of 2.2. This material was chosen to make the widths and spacings of the coupled sections realizable.

A schematic diagram for the balanced oscillator is shown in Fig. 6. For a push–pull oscillator, we choose the stopbands of the antenna to occur in the odd mode only, and

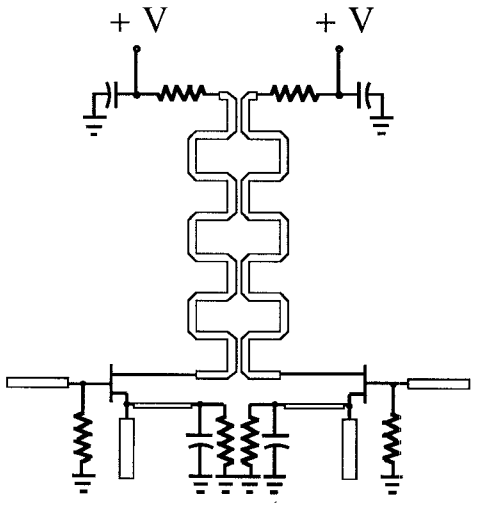

Fig. 6. Schematic view of balanced oscillator circuit.

by terminating the gates of the FET's using $\lambda/4$ open circuit stubs, cause the oscillation condition to be satisfied at a frequency such that the distance between the centers of the miters is equal to $\lambda/4$. In this situation, the radiation occurs at the fundamental frequency.

The coupled antennas for both the push–pull and push–push circuits were designed using Touchstone by separately considering the even and odd modes of excitation. For the push–pull case, the odd-mode behavior of the antenna was modeled as a concatenation of $3\lambda/4$ sections of 50 Ω ideal transmission line with $\lambda/4$ sections of line with impedance of less than 50 Ω. The impedance of the $\lambda/4$ sections was then varied until the desired combination of stopband height and passband *VSWR* was achieved. The coupled microstrip sections were then synthesized so that the odd-mode impedance would be equal to that of the $\lambda/4$ sections from the ideal case, while the even-mode impedance was equal to 50 Ω. For a typical nine-section antenna, the values of the odd-mode impedance varied from 34.5 Ω for the centermost element to 42 Ω for the end sections. This corresponds to width = 74.7 mils and spacing = 7.3 mils for the centermost section and width = 69.4 mils and spacing = 27.1 mils for the end sections.

Once the impedance values for the coupled sections are determined, the radiation patterns for the antenna may be predicted. As shown in [13], for the rampart line antenna, the radiation may be considered to arise from the fringing fields at the mitered bends. For an approximate analysis, we model these fringing fields as infinitesimal magnetic dipoles above a perfectly conducting ground plane. We expect that this approximation will be most valid for angles near broadside, and in the plane that contains the axis of the antenna.

The weighting for the infinitesimal dipoles is given by the voltages at the mitered bends. These voltages may be expressed in terms of the odd-mode impedances of the coupled sections by making an imaginary cut at the location of the bend and replacing the circuit on each side of the cut by its Thevenin equivalent. At the desired oscillation frequency, each section of the rampart line is $\lambda/4$ long, which simplifies the expressions. If we number the sections as shown in Fig. 7, we may then identify each mitered bend with a pair of indices, the first indicating a section, and the second running from 1 to 4 to indicate one of the four corners in each section. Using this notation, we may derive the following expressions for the voltage at the nodes in the nth section:

$$V_{n,1} = -jD^{-1}Z_T \prod_{i=1}^{n-1} Z_i$$

$$V_{n,2} = -D^{-1} \prod_{i=1}^{N} Z_i^2 \prod_{i=1}^{n-1} Z_i^{-1}$$

$$V_{n,3} = -V_{n,1}$$

$$V_{n,4} = -V_{n,2}$$

where Z_i is the odd-mode impedance of the ith coupled section, Z_T is the termination impedance, Z_S is the source impedance, N is the total number of coupled sections, j is the square root of -1, and

$$D = Z_T Z_S + \prod_{i=1}^{N} Z_i^2.$$

All impedances are normalized. The above expressions assume that the electrical distances between bends are exactly $\lambda/4$, and neglect the length of the mitered bend itself.

For a push–push oscillator the same method is used, except that the coupled sections are chosen such that $Z_{0o} = Z_0$ and $Z_{0e} > Z_0$, so that the devices oscillate in the even mode. In this case, radiation at the fundamental frequency is suppressed, and the antenna will radiate the second-harmonic component of the oscillation. This configuration is used for frequency doubling. In this case, for a typical nine-element antenna, the even-mode impedance of the centermost coupled section was 64 Ω, while for the end sections it was 55 Ω. This corresponds to width = 42 mils and spacing = 10.5 mils for the centermost section and width = 56.7 mils and spacing = 50 mils for the end sections.

For second-harmonic excitation, the mitered bends are separated by $\lambda/2$ sections of transmission line, so that in this case we may assume uniform illumination along the structure, to a first approximation.

IV. Transceiver Design

The oscillator circuits described above require only a slight modification for use as transceiver circuits, where the FET's perform a dual function, serving as the source for the transmitted signal and as self-oscillating mixers for down-conversion of the received signal. A more detailed account appears in [14].

A. Single-Device Transceiver

A single-device transceiver may be constructed by adding an IF transformer to the drain of the circuit in Fig. 4, resulting in the circuit shown in Fig. 8. In this case, the

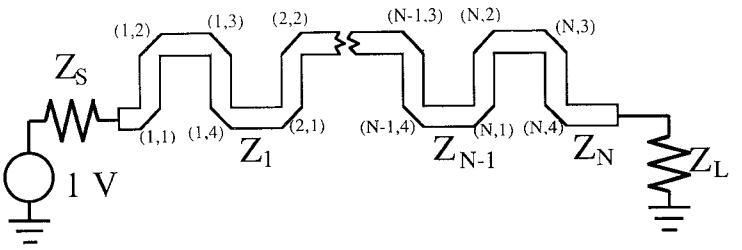

Fig. 7. Indexing system for mitered bends.

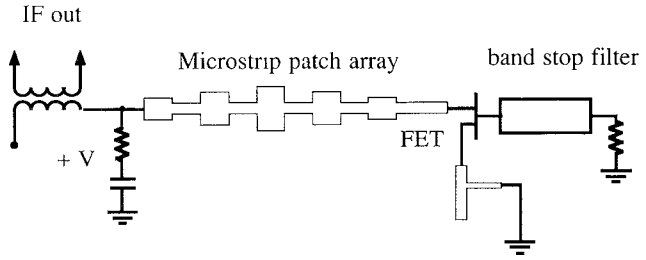

Fig 8. Schematic view of single-device transceiver circuit.

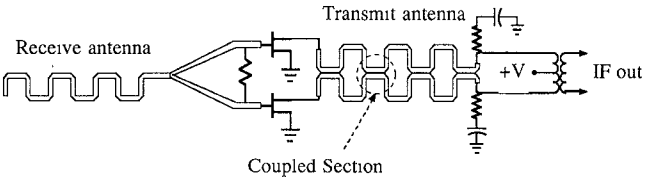

Fig. 9. Schematic view of balanced transceiver circuit.

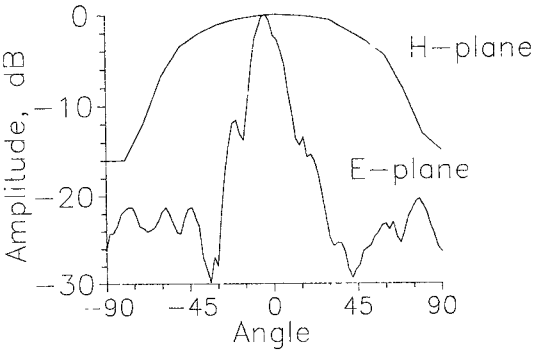

Fig. 10. Radiation patterns for single-device oscillator with 17-element antenna.

received signal is injected to the drain of the FET, from which the IF is also extracted. Since the received and transmitted signals are polarized in the same direction, this circuit may be used as a Doppler transceiver module. In this case, the IF transformer must function at audio frequencies.

It is possible to inject the received signal to the gate of the FET by using a separate receive antenna at the gate. In this case, the receive antenna must also perform the function of the low-pass or band-stop filter shown in Fig. 4.

B. Balanced Transceiver

The balanced transceiver we describe here is constructed from the balanced oscillator in which the FET's oscillate in the odd mode. It is similar in operation to the single-device design, except that a 180° hybrid must be added to the IF circuit to combine the IF signals from the two FET's.

The received signal may be injected to the gates of the FET's in the even mode using a separate antenna, as shown in Fig. 9. In this way, the receive antenna may be isolated from the resonant circuit, which operates in the odd mode. This allows a great deal of flexibility in the design of the receive antenna. For example, the receive antenna may be polarized perpendicularly to the transmit antenna, to isolate the two signals, or in the same direction for use in Doppler systems.

V. Prototype Circuits

Prototype circuits were constructed using packaged NE71083 small-signal FET's manufactured by NEC. The circuits were designed to oscillate at *X*-band in the vicinity of 10 GHz. The circuits were constructed using Duroid soft substrate from Rogers, Inc. For the single-device circuits, the relative dielectric constant was 10.2 with a thickness of 25 mils; for the balanced circuits, the relative dielectric constant was 2.2 with a thickness of 20 mils. The Touchstone microwave CAD program from EEsof was used in the design of all circuits. In order to keep the construction of the circuits manageable, their overall lengths were held below 8 in.

VI. Experimental Results

A. Sources

The radiation pattern for a single-device oscillator using a 17-element patch array is shown in Fig. 10, with the output power and frequency versus V_{gs} shown in Fig. 11. In this case, the overall length of the antenna is 6.8 in. The operating frequency is 9.5 GHz.

Figs. 12 and 13 show the calculated and measured performance of a push–pull oscillator with an antenna composed of nine coupled sections as described above, with an overall length of 4.2 in. The calculated and measured results agree reasonably well in the *H*-plane case for angles near to normal. For the *E*-plane patterns, the element factor for the individual mitered bends has a more noticeable effect on the overall pattern. The lobes in the *E*-plane pattern are due to the effect of the finite ground plane of the circuit. Not shown are the cross-polarized fields, which are more than 20 dB below the main lobe for both the *E* and the *H* plane. Our simple model overestimates the cross-polarization levels by 7 dB for the *E* plane but predicts no cross-polarization for the *H* plane. The

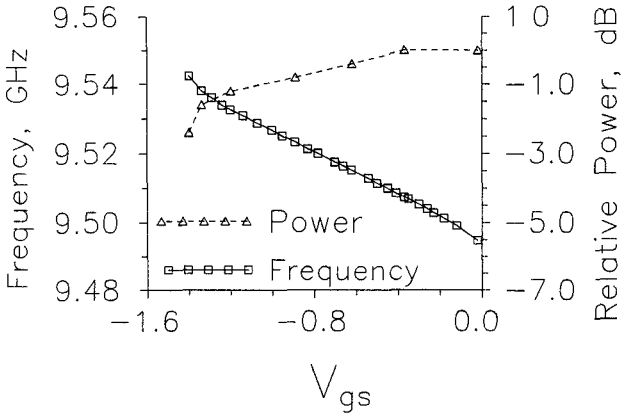

Fig. 11. Oscillation frequency and relative output power for the single-device oscillator.

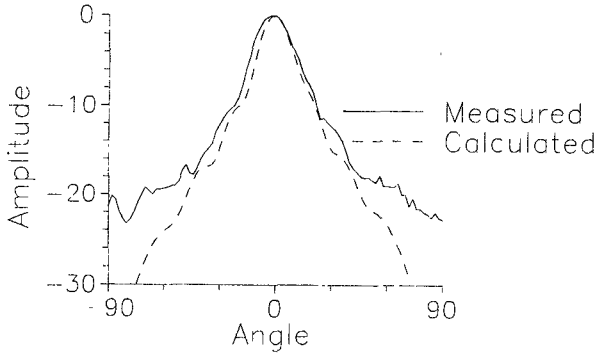

Fig. 12. *H*-plane radiation pattern for the push–pull oscillator.

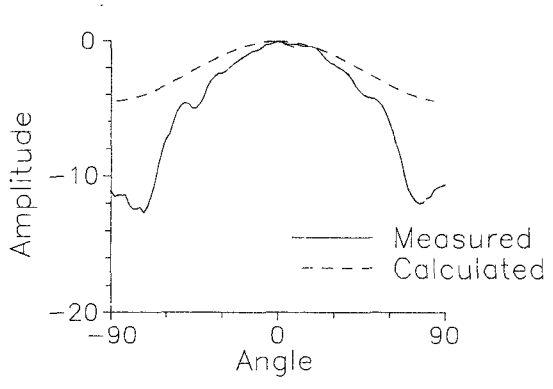

Fig. 13. *E*-plane radiation pattern for the push–pull oscillator.

agreement between our predicted and measured patterns indicates that the radiation from the remainder of the circuit, such as the gate and source circuits, is not a great problem.

For quasi-optical oscillators we may define an isotropic dc–RF conversion gain as the ratio of transmitted power in a particular direction to that of an isotropic source radiating with 100 percent dc–RF conversion efficiency [15]. Defined in this way, the effective radiated power (*ERP*) is equal to the product of isotropic dc–RF conversion efficiency and dc bias power.

The isotropic dc–RF conversion efficiency is measured by comparing the output of a standard gain horn driven with a known RF power to that of the oscillator. Since the

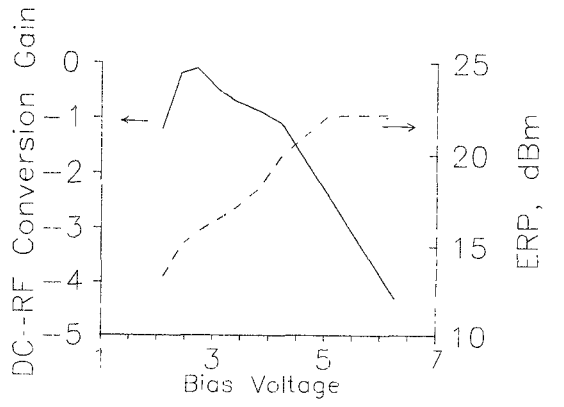

Fig. 14. Isotropic second-harmonic conversion efficiency and *ERP* for the push–push oscillator.

efficiency of the oscillator is a function of bias point, the isotropic dc–RF conversion efficiency also varies with bias. For the single-device oscillator we measure a 9 dB isotropic dc–RF conversion gain in the broadside direction. For the balanced oscillator, the measured value is 6.1 dB. These are maximum values over a range of operating points. The values of effective radiated power for these operating points are 31.6 dBm and 29.0 dBm, respectively.

B. Frequency-Doubling Source

By operating the balanced oscillator in the push–push mode, a frequency-doubling planar source was created which radiated the second harmonic at 19.7 GHz. A plot of second-harmonic dc–RF conversion gain and *ERP* is shown in Fig. 14, for a push–push oscillator using a nine-element coupled rampart line antenna, with an overall length of 4.2 in.

As is typical of push–push oscillators, the fundamental signal was also present with a broad radiation pattern, presumably due to radiation from the FET's and tuning elements. For the range of operating points shown in Fig. 12, the fundamental signal in the broadside direction was within 2 dB above or below that of the main second-harmonic lobe.

C. Transceivers

Single-device and balanced transceivers of the type shown in Figs. 7 and 8 were constructed and tested. For the balanced structure, the receive antenna was configured so that the received polarization was the same as the transmitted signal, to allow its use as a Doppler module. Transmit and receive patterns for the single-device transceiver with a 12-element patch antenna are shown in Figs. 15 and 16; those for a balanced circuit with a five-element coupled transmit antenna and an eight-element single rampart line receive antenna are shown in Figs. 17 and 18. The single-device transceiver exhibits a narrower tuning bandwidth due to the fact that it uses a higher Q band-stop filter on the gate.

For quasi-optical transceivers, we may define an isotropic receiver gain as the ratio of IF power to that of an isotropic receiver with 100 percent RF–IF conversion

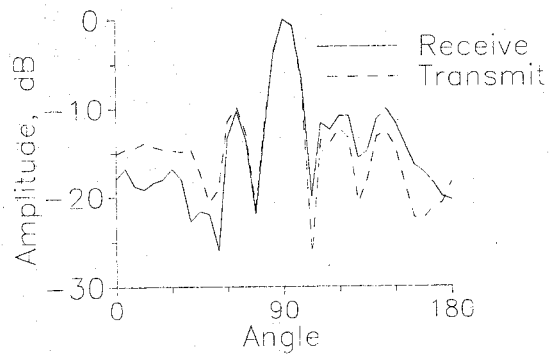

Fig. 15. *E*-plane transmit and receive patterns for the single-device transceiver.

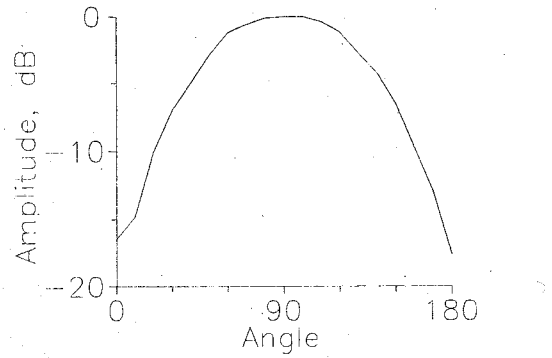

Fig. 16. *H*-plane transmit pattern for the single-device transceiver.

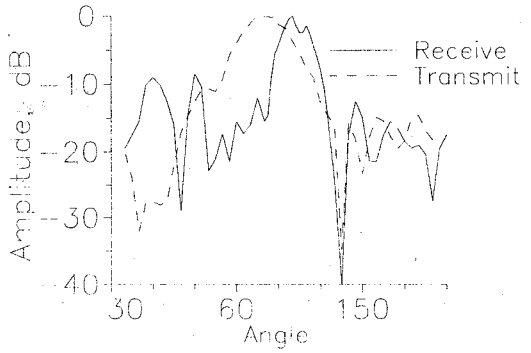

Fig. 17. *H*-plane transmit and receive patterns for the balanced transceiver.

efficiency [16]. Table I shows isotropic dc–RF conversion gain, receiver gain, and *ERP* for the two prototype circuits. The gains shown were measured for an IF frequency of approximately 10 MHz. It should be mentioned that the receiver gain was a maximum at very low bias levels, near the onset of oscillation. At such low bias levels, the operation of the device may not be stable with respect to temperature or other factors; therefore it may be necessary to forgo high-gain operation in favor of operating at a more stable bias point.

Due to the size restrictions on the circuits, the balanced transceiver circuit employed a much shorter resonant antenna than the other circuits. For this reason, the stopband of the resonant antenna is much broader, allowing the circuit to oscillate rather far from the design frequency of

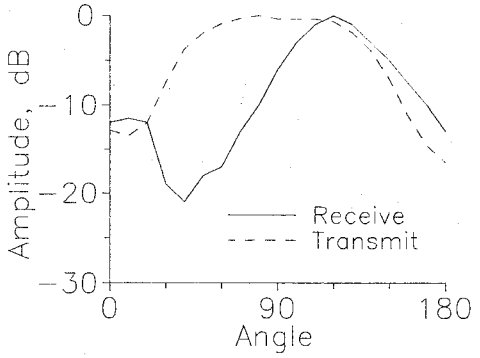

Fig. 18. *E*-plane transmit and receive patterns for the balanced transceiver.

TABLE I
ISOTROPIC DC–RF CONVERSION GAIN, RECEIVER GAIN, AND *ERP* FOR THE PROTOTYPE CIRCUITS

	Maximum dc-rf isotropic conversion gain		Maximum isotropic receiver gain		Maximum ERP	
	Value	dc bias	Value	dc bias	Value	dc bias
Single Device Oscillator	2.5 dB	4.4 V	8.8 dB	2.2 V	24.9 dBm	4.4 V
Balanced Oscillator	5.5 dB	1.6 V	2.7 dB	1.05 V	24.5 dBm	3.0 V

10 GHz. Since both the angle of the radiation maximum and the antenna gain are dependent on operating frequency for this type of structure, the balanced transceiver exhibits lower conversion gain and is somewhat "cross-eyed." The use of longer transmit and receive antennas obviates this problem.

It was noted during testing of the transceiver circuits that the highest conversion gain occurred when the received signal was near the transmit signal. Above an IF frequency of about 20 MHz, the receiver gain dropped considerably. This type of behavior is acceptable for Doppler applications where the IF bandwidth requirements are quite low.

A qualitative demonstration of the use of these transceiver modules for Doppler motion detection was undertaken. By coupling the IF signal out through an audio transformer and displaying the signal on an oscilloscope, the response of the circuit to motion in the vicinity could be displayed. It was discovered that using this crude instrumentation, the motion of a person walking within 10 to 20 ft of the module was easily detected. This performance could no doubt be improved with a carefully designed IF amplifier circuit.

VII. CONCLUSIONS

The circuits reported here have many applications as single units for communications and radar purposes. In addition, each is suitable as an element of a phased array

in an active antenna configuration or in a quasi-optical power-combining scheme. The latter approach is generally used at millimeter-wave frequencies, where planar arrays of such sources are used to combine power into beam wave modes.

Of particular interest for millimeter-wave quasi-optical systems is the push–push second-harmonic oscillator. A planar array of these elements injection locked at the fundamental frequency can be used as an active frequency doubler in conjunction with a grid for separation of the fundamental and second harmonic.

Finally, the planar transceivers have exhibited the potential for application to Doppler motion detection systems, where they exhibit significant advantages over conventional systems in size, weight, and power consumption.

ACKNOWLEDGMENT

The authors would like to thank Dr. D. P. Neikirk and the Microelectronics Research Center of The University of Texas at Austin for providing the equipment used for circuit fabrication.

REFERENCES

[1] J. W. Mink, "Quasi-optical power combining of solid-state millimeter-wave sources," *IEEE Trans. Microwave Theory Tech.*, vol. MTT-34, pp. 273–279, 1986.

[2] Z. B. Popovic, M. Kim, and D. B. Rutledge, "Grid oscillators," *Int. J. Infrared and Millimeter-Waves*, vol. 9, pp. 647–654, 1988.

[3] D. B. Rutledge, Z. B. Popovic, and M. Kim, "Millimeter-wave grid oscillators," in *Proc. 13th Int. Conf. Infrared and Millimeter-Waves* (Honolulu), Dec. 1988, pp. 1–2.

[4] C. M. Jackson, J. A. Lester, M. A. Yu, and Y. C. Ngan, "Quasi-optical patch mixers at 35 and 94 GHz," in *1988 IEEE MTT-S Int. Microwave Symp. Dig.* (New York), pp. 781–784.

[5] N. Camilleri and B. Bayraktaroglu, "Monolithic millimeter wave IMPATT oscillator and active antenna," in *1988 IEEE MTT-S Int. Microwave Symp. Dig.* (New York), pp. 955–958.

[6] K. A. Hummer and K. Chang, "Microstrip active antennas and arrays," in *1988 IEEE MTT-S Int. Microwave Symp. Dig.* (New York), pp. 955–958.

[7] K. D. Stephan, "Inter-injection-locked oscillators for power combining and phased arrays," *IEEE Trans. Microwave Theory Tech.*, vol. MTT-34, pp. 1017–1025, 1986.

[8] B.-S. Song and T. Itoh, "Distributed Bragg reflection dielectric waveguide oscillators," *IEEE Trans. Microwave Theory Tech.*, vol. MTT-27, pp. 1019–1022, 1979.

[9] R. E. Collin and F. J. Zucker, *Antenna Theory*. New York: Wiley, 1969, pt. II, ch. 19.

[10] J. Birkeland and T. Itoh, "Planar FET oscillators using periodic microstrip patch antennas," *IEEE Trans. Microwave Theory Tech.*, vol. 37, pp. 1232–1236, Aug. 1989.

[11] I. J. Bahl and P. Bhartia, *Microstrip Antennas*. Dedham, MA: Artech House, 1980, ch. 2.

[12] J. Birkeland and T. Itoh, "Power combining FET oscillators using coupled rampart line antennas," in *Proc. 13th Int. Conf. Infrared Millimeter Waves* (Honolulu), Dec. 1988, pp. 5–6.

[13] P. S. Hall, "Microstrip linear array with polarization control," *Proc. Inst. Elec. Eng.*, vol. 130, pt. H, no. 3, pp. 215–224, 1983.

[14] J. Birkeland and T. Itoh, "Quasi-optical planar FET transceiver modules," to appear in *1989 IEEE MTT-S Int. Microwave Symp.* (Long Beach).

[15] S. Nam, T. Uwano, and T. Itoh, "Microstrip-fed planar frequency-multiplying space combiner," *IEEE Trans. Microwave Theory Tech.*, vol. MTT-35, pp. 1271–1276, 1987.

[16] K. D. Stephan and T. Itoh, "A planar quasi-optical subharmonically pumped mixer characterized by isotropic conversion loss," *IEEE Trans. Microwave Theory Tech.*, vol. MTT-32, pp. 97–102, 1984.

✠

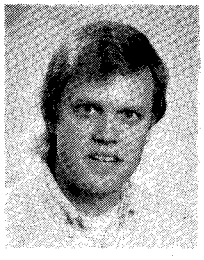

Joel Birkeland (S'87) received the B.S. degree in physics from Oregon State University in 1982, and the M.S.E. in electrical engineering from Arizona State University in 1985.

From February 1985 to August 1987 he was employed at M/A-COM Active Assemblies Division in Tempe, AZ, where he worked on low-noise hybrid microwave amplifiers. In September 1987 he entered the Ph.D. program in electrical engineering at the University of Texas at Austin on a University Fellowship. Mr. Birkeland was the recipient of an MTT-S Fellowship for 1989.

✠

Tatsuo Itoh (S'69–M'69–SM'74–F'82) received the Ph.D. degree in electrical engineering from the University of Illinois, Urbana, in 1969.

From September 1966 to April 1976, he was with the Electrical Engineering Department, University of Illinois. From April 1976 to August 1977, he was a Senior Research Engineer in the Radio Physics Laboratory, SRI International, Menlo Park, CA. From August 1977 to June 1978, he was an Associate Professor at the University of Kentucky, Lexington. In July 1978, he joined the faculty at the University of Texas at Austin, where he is now a Professor of Electrical Engineering and Director of the Electrical Engineering Research Laboratory. During the summer of 1979, he was a guest researcher at AEG-Telefunken, Ulm, West Germany. Since September 1983, he has held the Hayden Head Centennial Professorship of Engineering at the University of Texas. In September 1984, he was appointed Associate Chairman for Research and Planning of the Electrical and Computer Engineering Department. He also holds an Honorary Visiting Professorship at the Nanjing Institute of Technology, China.

Dr. Itoh is a member of Sigma Xi and of the Institute of Electronics and Communication Engineers of Japan. He is a member of Commission B and Chairman of Commission D of USNC/URSI. He served as the Editor of the IEEE TRANSACTIONS ON MICROWAVE THEORY AND TECHNIQUES for 1983–1985. He serves on the Administrative Committee of the IEEE Microwave Theory and Techniques Society. Dr. Itoh is a Professional Engineer registered in the state of Texas.